RSC Applied Interfaces

ROYAL SOCIETY OF CHEMISTRY

PAPER

View Article Online
View Journal | View Issue

Cite this: *RSC Appl. Interfaces*, 2025, **2**, 755

Enabling hydrogel coating on silicone breast implants with a poly(vinyl acetate) primer layer†

Katrin Stanger,‡[a] Dardan Bajrami,‡[bc] Peter Wahl,[de] Fintan Moriarty,[f] Emanuel Gautier,[gh] Alex Dommann[i] and Kongchang Wei*[bj]

Implant-associated infection is a major cause for breast implant re-operation. A practical method to reduce this risk is yet to be established. Hydrogel coating represents one promising approach. However, the adhesion of the hydrogel layer onto the silicone implant surface presents a significant challenge due to the intrinsic hydrophobicity of silicone surfaces. In this study, we described a surface-priming strategy involving poly(vinyl acetate) (PVAc) polymers to facilitate hydrogel adhesion to silicone implant surfaces. Miniature silicone implants with identical surface properties to clinical implants were custom-made for this study. We demonstrated that a PVAc primer layer can easily be deposited on the implant surface *via* a dip-coating procedure. The wettability of the implant surface was increased by a stable and cytocompatible primer layer of PVAc. The improved wettability allowed the application of a model hydrogel precursor solution (alginate) on the primed implant surface. The effectiveness of such a priming strategy in facilitating hydrogel coatings was validated by testing two commercially available hydrogels on the silicone implant surface. Specifically, DAC (defensive antibacterial coating) and Coseal hydrogels, representing paintable and sprayable hydrogels, respectively, were successfully coated on the primed surface, as confirmed by ATR-FTIR analysis. Our surface-priming strategy, which avoids surface treatments like chemical reactions and plasma irradiation that are impractical for clinical use, opens up new opportunities for exploring intraoperative hydrogel applications on silicone implants.

Received 22nd August 2024,
Accepted 16th February 2025

DOI: 10.1039/d4lf00301b

rsc.li/RSCApplInter

Introduction

Silicone breast implants have been engineered not only for aesthetic reasons for breast augmentation, but also for reconstructive purposes after surgical breast cancer treatment.[1,2] The number of implantations is increasing tremendously.[3] However, up to 41% of the implants need re-operation, either for overt septic reasons or due to capsular fibrosis, which is most likely due to low-grade infections.[4–6] Reported incidence of infection ranges from less than 10% to over 60%.[4–6] Alternatives for breast reconstruction after mastectomy include technically challenging operations, such as microsurgical autologous free flap transplantation. However, these operations bear major morbidity and complication rates.[7] Reconstruction of the breast with silicone implants is a preferable alternative because of technical simplicity, quicker recovery time, and enhanced aesthetic outcome.[8]

Implants are most susceptible to colonization by microorganisms at implantation or within the following hours.[9,10] Treatment of established implant-associated infections is expensive and cumbersome, varying from long-term antibiotic therapy to surgical debridement and implant replacement.[11] Thus, preventing intraoperative contamination is essential.[12] Altering the surface properties of the implant has been demonstrated to be an effective approach to reduce the risk of post-implantation complications.[13–15] Such surface modifications include coatings with antimicrobial agents,[16,17] nanomaterials,[18,19] adhesive interfaces,[20] and plasma-induced chemical changes of molecular structures.[21,22]

[a] *Division of Plastic and Hand Surgery, Cantonal Hospital Winterthur, Winterthur, Switzerland*
[b] *Empa, Swiss Federal Laboratories for Materials Science and Technology, Laboratory for Biomimetic Membranes and Textiles, Lerchenfeldstrasse 5, 9014 St. Gallen, Switzerland. E-mail: kongchang.wei@empa.ch*
[c] *ZHAW School of Engineering, Technikumstrasse 71, Winterthur, Switzerland*
[d] *Division of Orthopaedics and Traumatology, Cantonal Hospital Winterthur, Winterthur, Switzerland*
[e] *Faculty of Medicine, University of Bern, Bern, Switzerland*
[f] *AO Research Institute Davos, Davos, Switzerland*
[g] *Department of Orthopaedics, HFR Fribourg – Cantonal Hospital, Fribourg, Switzerland*
[h] *OrthoTrauma Foundation, Fribourg, Switzerland*
[i] *ARTORG Center for Biomedical Engineering Research, University of Bern, Bern, Switzerland*
[j] *Empa, Swiss Federal Laboratories for Materials Science and Technology, Laboratory for Biointerfaces, Lerchenfeldstrasse 5, 9014 St. Gallen, Switzerland*
† Electronic supplementary information (ESI) available. See DOI: **https://doi.org/10.1039/d4lf00301b**
‡ These two authors contributed equally to this work.

As water-retaining soft materials made from hydrophilic polymers,[23] hydrogels have been shown to be promising in preventing bacterial adhesion at an early stage of infection, for instance, of wounds and bone implants.[23–30] Before degradation, they can hinder adherence of microorganisms on the surface of the implant just long enough for the immune system to eliminate any intraoperative contaminant and thus prevent biofilm formation and development of infection.[31–34] Recent studies have demonstrated the effectiveness of hydrogel coatings in preventing biofilm development on joint replacement and fracture-fixation implants, highlighting the potential clinical utility of this approach for improving patient outcomes in breast implant surgery.[29,35–37] Silicone breast implants are particularly well suited for applying a dissolving coating like hydrogels, as they require no tissue integration for proper functioning.

The key challenge for coating silicone breast implants with hydrogels is the poor surface wettability of such hydrophobic materials.[38] Various strategies have been explored to improve wettability, including surface activation and oxidation to modify the surface polarity.[39] However, such methods rely on the alteration of surface chemical structures, which could potentially raise safety concerns, as well as challenges in meeting product integrity and regulatory standards. Therefore, there is a need for easily applicable, yet effective approaches for improving silicone implant wettability. Recently, Cheng *et al.* utilized poly(vinyl acetate) (PVAc) as a primer layer between silicone rubber and an *in situ* formed tough hydrogel to achieve a hydrogel coating *via* photo-initiated grafting.[40] The PVAc layer served as a bridging matrix to immobilize the tough hydrogel, formed by polymerization of synthetic monomers in the presence of initiators and crosslinkers.[40] Due to its biocompatibility and biodegradability, PVAc has been used in various biomedical applications.[41–43] Such a surface-priming strategy offers a straightforward approach to bond *in situ* formed hydrogels to silicone rubber surfaces, without altering its molecular structure. Its effectiveness for the application of commercially available hydrogels for implantation on silicone implant surfaces is, however, yet to be verified. In this study, we explored the application of a PVAc primer layer in improving the wettability of silicone breast implant surfaces. Successful coating of commercially available hydrogels of different types, namely, a paintable physical hydrogel (DAC) and a sprayable chemical hydrogel (Coseal), on PVAc-primed implants was demonstrated, without involving additional chemicals (*e.g.* initiators and crosslinkers),[40] thus providing a promising approach in the operation room to use hydrogels as coatings of silicone implants for prevention of infection.

Materials and methods

Materials

Silicone implants corresponding to clinical breast augmentation implants (Motiva Implants with SmoothSilk surface, Establishment Labs Holdings Inc., Alajuela, Costa Rica) were miniaturized to a diameter of 15 mm and a height of 5 mm (Fig. 1A-a), and then tested by the manufacturer following ISO-14607:2018 TS-17-026.R (Rheology Testing of Breast Implant Gels with the BTC-2000). The core is made of heated liquid silicone, which turns into a soft jellylike material with high viscoelasticity and cohesive strength after

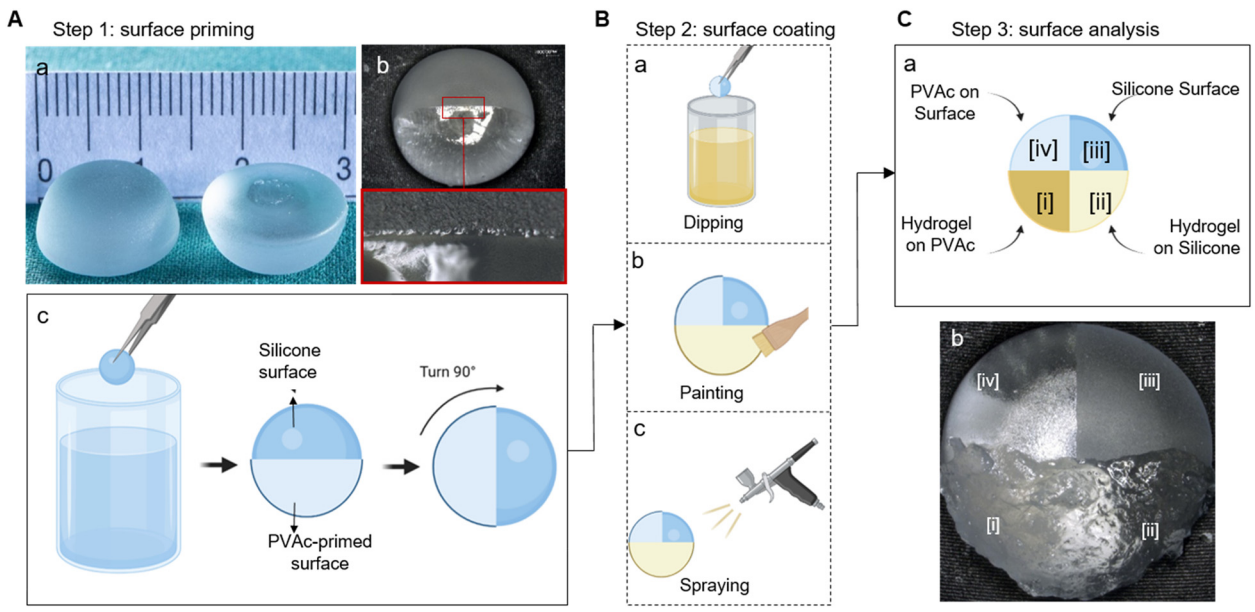

Fig. 1 Surface priming, coating and analysis of miniaturized silicone breast implants. A-a: Custom-made silicone implants. A-b: Half of the implant primed with PVAc (upper) and the boundary between the PVAc-primed and the original implant surface; A-c: PVAc coating process by dipping and rotation of the implant for the further coating process. B: Three different surface coating processes for subsequent coatings of implants with the alginate solution (a), DAC (b), and Coseal (c). C-a: Implant samples with four zones for the analysis; C-b: a representative microscopy image of the coated implant with four different zones (zones [i] and [ii] were coated with DAC, [iii] and [iv] as indicated in paneal C-a).

cooling. The surface is made of polymerized nanotextured silicone. Sodium alginate (Sigma Aldrich, St. Louis, MO, USA, Mw. 20 kDa) was dissolved in deionized (DI) water at room temperature (23 °C) under stirring to give a 5 wt% solution. Poly(vinyl acetate) (PVAc, Mw. 100 kDa, Sigma Aldrich) was dissolved in acetone at 40 °C under stirring to give a 2 wt% solution. Defensive antibacterial coating (DAC, Novagenit, Mezzolombardo, Italy) and Coseal surgical sealant (Baxter, Glattpark, Switzerland) were used as purchased (without additional drug loading). DAC is composed of hyaluronic acid (HA) and poly-D,L-lactide (PDLLA), while Coseal is composed of two different functionalized poly(ethylene glycol) (PEG) polymers, namely, tetra-NHS-derivatized PEG and tetra-thiol-derivatized PEG.[36]

Methods

Surface priming

The implants were thoroughly cleaned by using a stepwise process. They were firstly soaked in acetone and isopropanol for 10 minutes each and then cleaned by ultrasonication in deionized water for 10 minutes. After drying at room temperature in air, the implants were partially dipped into the PVAc solution for 3 seconds, followed by 15 minutes drying in air. This dipping–drying cycle was repeated 3 times, as illustrated in Fig. 1A-a. The coating weight was determined by measuring the implant mass before and after the coating process, with an average coating weight of approximately 18.95 mg (±30.42 mg). The samples were subjected to surface analysis after drying in air for 1 h.

Swelling and degradation

PVAc-primed implants were weighed to determine their initial dry weight (W_0). Subsequently, they were immersed in phosphate-buffered saline (PBS, 37 °C) for 7 days. After this period, the implants were removed from PBS and gently patted dry to remove the excess liquid before determining their wet weight after PVAc swelling (W_s). The implants were allowed to dry at room temperature for 24 hours before being weighed for the dry weight after degradation (W_d). The swelling ratio (SR) and degradation fraction (DF) were calculated as below.

$$\text{SR } \% = 100 \times (W_s - W_0)/W_0$$

$$\text{DF } \% = 100 \times (W_d - W_0)/W_0$$

Cytotoxicity test using an MTS assay

PVAc samples were prepared and tested according to ISO 10993-12 "Biological evaluation of medical devices, Part 12: Sample preparation and reference materials" and ISO 10993-5:2009 "Biological evaluation of medical devices, Part 5: Tests for in vitro cytotoxicity", respectively. Specifically, PVAc thin layers (sterilized under UV irradiation) were immersed in complete growth media (DMEM supplemented with 10% FBS and 1% P/S) at an extraction ratio of 0.1 g mL^{-1} for 24 h at 37 °C with continuous movement to gain the conditioned media. Human dermal fibroblasts (HDFs; passage 6) were seeded at 5000 cells per well in 96-well plates (TPP, lot. 92096). With a final volume of 100 μL of complete growth media, the cells were cultured for 24 h at 37 °C in 5% CO_2 to get a semi-confluent monolayer before switching to the conditioned media. The cytotoxicity was assessed using the CellTiter 96® AQueous One Solution Cell Proliferation Assay (MTS) after 3 days following the manufacturer's instructions. A freshly prepared dye solution (MTS reagent) was added to each well together with the RPMI medium, and the absorbance was recorded at 490 nm using a 96-well plate reader (BioTek Synergy H1, Agilent Technologies, Santa Clara, California). Cell viability was normalized to cells cultured in standard complete growth media (negative control). Triton X-100 (Sigma Aldrich) at 1 wt% in PBS was used to induce cell death as the positive control.

Surface coating

Two commercially available hydrogels were tested on the PVAc-primed implants. The DAC hydrogel was applied to the implants using the manufacturer's applicator (Fig. 1B-b). The Coseal hydrogel was sprayed onto the implants using a spraying system provided by the manufacturer (Fig. 1B-c). The spraying was controlled by covering the areas that were not to be treated. In order to analyze the coating performance on surfaces with different features, the coating process was designed as illustrated in Fig. 1C.

Surface analysis

Contact angle measurements on the original implant surface and PVAc-primed implant surface were conducted by using a drop-shaped analyser (DSA25E, KRÜSS, Hamburg, Germany) at 23 °C temperature. The implants coated with the alginate solution were examined under an optical microscope (VHX-1000, Keyence, Osaka, Japan) and photographed at 10 second intervals to assess the solution's flow behavior. The implants coated with DAC and Coseal hydrogels were washed twice in phosphate-buffered saline (PBS, 0.01 M; Sigma Aldrich). Microscopic images were taken after each washing step. One hour after coating, the individual surface zones of all samples were characterized by Attenuated Total Reflectance Fourier-Transform Infrared spectroscopy (ATR-FTIR) (Varian 640-IR, Agilent Technologies, Santa Clara, USA). The dipping method chosen provides 4 zones (i: hydrogel on PVAc; ii: hydrogel on native silicone; iii: uncoated native silicone; iv: PVAc-primed silicone) on the surface of each implant (Fig. 1C), allowing direct comparison of the coatings.

Results and discussion

PVAc primer layer alters silicone surface properties

A hydrogel directly applied on the silicone implant leads to immediate retraction (ESI,† Fig. S1). This is due to the low wettability between the silicone surface and aqueous

solutions.[38] To improve wettability, we enhanced the hydrophilic surface properties by application of a PVAc primer layer on the silicone surface. To achieve comprehensive coverage over the inherently rough implant surface, the dip-coating process was repeated three times. The PVAc primer layer showed a smooth coverage on the implant surface without disruption (Fig. 1A-b). Using fewer layers resulted in inadequate coverage, which caused hydrophobic rejection of the subsequently applied hydrogel layer (ESI,† Fig. S2). The improved wettability of the PVAc-primed implant surface was revealed by contact angle measurements (Fig. 2A). The untreated silicone implant (−PVAc sample) exhibited a contact angle of 107.3 ± 12.4°, indicating a hydrophobic surface. In contrast, the PVAc-primed silicone implant surface (+PVAc sample) showed increased wettability, as evidenced by the significantly reduced contact angle of 62.3 ± 1.9°. The stability of the PVAc coating was assessed through swelling and degradation tests (Fig. 2B). The results indicated negligible swelling (<0.1%) and minimal degradation (<1.6%) of the PVAc coating after 1 week incubation in PBS (37 °C), confirming its robustness as a primer layer for further hydrogel coating application. FTIR analysis also confirmed the characteristic peaks of PVAc after this incubation (ESI,† Fig. S3).

Cytocompatibility of the PVAc primer layer

The cytotoxicity of PVAc was assessed by exposing human dermal fibroblasts (HDFs) to conditioned media derived from PVAc samples according to ISO 10993-"Biological Evaluation of Medical Devices". The results (Fig. 2C) of the MTS Assay (normalized to the negative group) showed that the cell viability in the PVAc conditioned media was 90.5 ± 4.8%. No significant decrease of cell viability was observed when compared to the negative control (neg.). In contrast, cell viability from the positive control group (pos.) was 1.9 ± 0.1%. This observation indicated the good cytocompatibility of the PVAc primer layer. In combination with its wettability and stability, the PVAc primer layer showed great potential in improving hydrogel coatings on silicone surfaces.

Subsequently, it was further validated by applying an alginate solution on both the primed and non-primed implant surfaces (Fig. 1B-a). Alginate is a natural polysaccharide found in brown algae, commonly used in wound dressings, tissue engineering, and drug delivery applications due to its biocompatibility, low toxicity, and gelation properties.[44] Therefore, alginate was selected herein to simulate the precursors of the commercially available hydrogels. It was observed that the alginate solution applied to the non-primed implant surfaces (−PVAc) suffered from rapid retraction, as did the hydrogels. The alginate solution was found retracted partially from the implant surface (zone [ii]) in the first 10 s after dip-coating (Fig. 3A). After two minutes, the alginate solution had almost entirely disengaged from the implant, with only the residual material remaining on the surface (Fig. 3B–D; ESI,† Movie S1). On the contrary, the alginate solution applied to the PVAc-primed surface (+PVAc) retained its position without any displacement or disintegration (Fig. 3D, zone [i]), thus confirming the bridging effect of the PVAc primer layer between the silicone surface and hydrogel precursor solutions.

The change of surface properties was characterized by ATR-FTIR analysis (Fig. 4). On the PVAc-primed surface (zone [i]), alginate-derived signals, including the O–H stretching vibrations caused by hydroxyl groups, intermolecular hydrogen bonding at 3200–3600 cm^{-1}, a sharp peak near 1600 cm^{-1} attributed to the asymmetric stretching of the carboxylate groups (COO–), and a sharp peak around 1030 cm^{-1}, typically associated with the C–O stretching vibrations,[45] were observed. On the contrary, the implant surface without the PVAc layer (zone [ii]) lacked such signals, confirming the poor adhesion between alginate and a native silicone surface. Specifically, the peaks at 1260 cm^{-1} (Si–CH_3 bending vibrations), 1010–1100 cm^{-1} (Si–O–Si stretching vibrations), and around 800 cm^{-1} (Si–C stretching vibration) revealed the bare silicone surface after unsuccessful alginate coating[45] (zone [ii]), which is in accordance with the signals from the reference surface (zone [iii]). Only alginate residues were detected on such non-primed surfaces, with peaks in the 3200–3600 cm^{-1} and 1600 cm^{-1} regions (zone [ii]). It is noteworthy that when the ATR-FTIR signals from zone [ii] were compared to those from

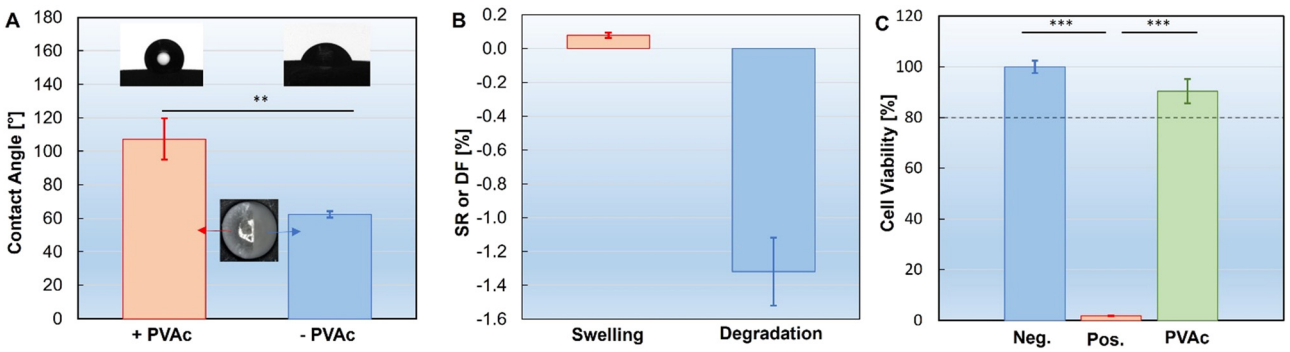

Fig. 2 (A) Contact angle measurements of PVAc-primed silicone implants (+PVAc) and the non-primed ones (−PVAc). (B) Swelling and degradation of the PVAc primer layer on silicone implants. Error bars represent the standard deviation of the measurements (n = 3, ** $p < 0.005$). (C) Viability of human dermal fibroblast (HDF, passage 6) cells cultured in conditioned media derived from PVAc. The graph shows significant cell proliferation in PVAc-treated groups (green bar) compared to the negative control (red bar) (n = 3, *** $p < 0.001$).

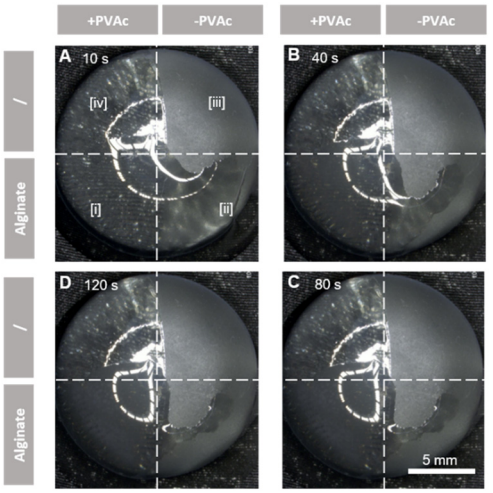

Fig. 3 PVAc primer layer alters silicone surface properties. Silicone implants were divided into four zones, visualized by dotted white lines. The images were taken at 10 s (A), 40 s (B), 80 s (C), and 120 s (D) after dipping the implants (zone [i] and [ii]) in the alginate solution.

zone [iii], a difference in the silicone-derived signal amplitude was obvious. This could be due to the change in the surface roughness and refractive index induced by the alginate residues on the zone [ii] surface. The native implant surface with higher roughness (zone [iii]) compromised the contact between the sample and the ATR crystal, leading to weaker signals from zone [iii] than zone [ii].

In addition, successful priming of the implant surface with PVAc was confirmed by signals at approximately 1730 cm^{-1} from zone [iv] attributed to the acetate's carbonyl, and around 1240 cm^{-1} attributed to the C–O stretching from the ester linkage, as well as peaks between 2800 and 3000 cm^{-1} for the alkyl groups (zone [iv]).

According to this analysis, we confirmed that a PVAc primer layer could be applied on silicone implant surfaces without alteration of the molecular structure, offering a praticable approach to improve the wettability of the implant surface for retention of applied aqueous solutions (*e.g.* hydrogel precursors). Compared to other surface treatments, such as chemical activation[40] and plasma treatment,[21,22] this PVAc priming approach represents a more feasible approach for intraoperative application on implants.

PVAc-mediated coating of silicone implants with a paintable hydrogel (DAC)

DAC is commercially available for implant surface coating, where it acts a physical barrier for infection prevention.[46] Unlike the liquid-form alginate precursor solution, DAC is a high-viscosity physical hydrogel, which cannot be applied to the implant surface by dip-coating. As instructed by the manufacturer, DAC was applied to the implant surface with the brush provided by the manufacturer.

Before coating, the PVAc primer layer showed a homogeneous and smooth surface (Fig. 5A, zone [iv]).

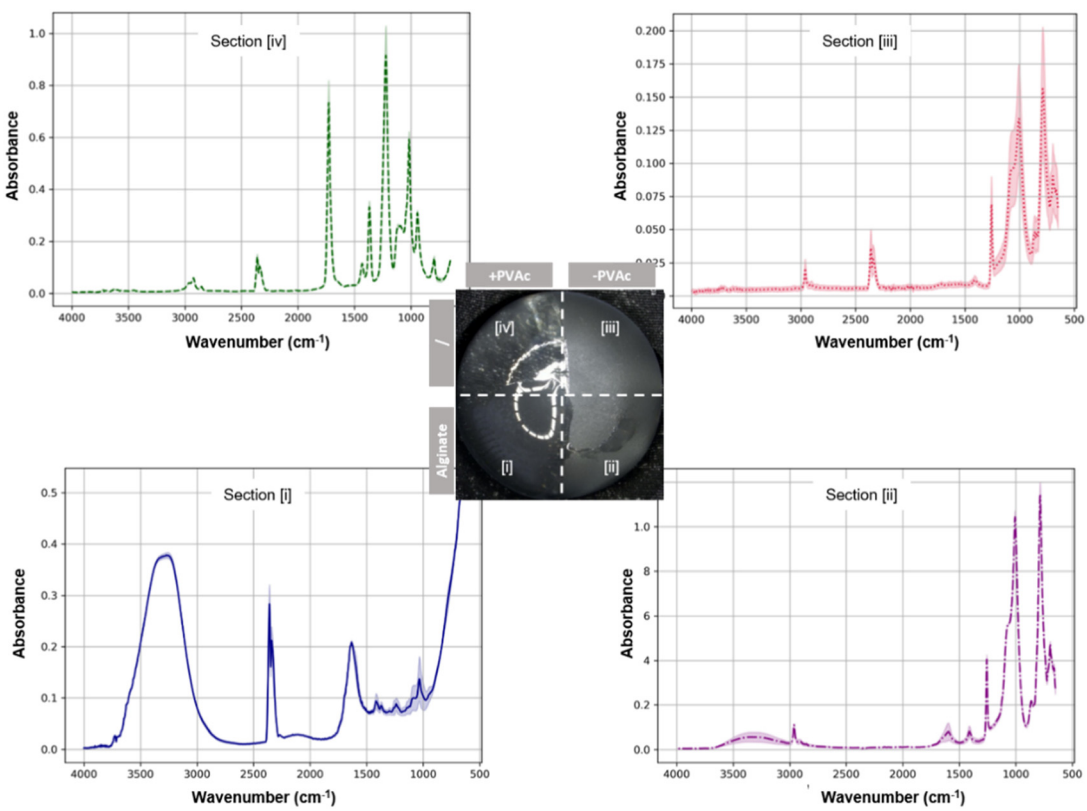

Fig. 4 ATR-FTIR spectra of different implant surface zones measured one hour after the alginate coating (n = 3).

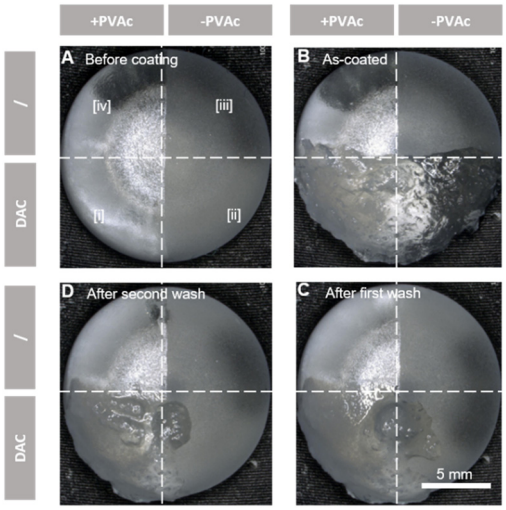

Fig. 5 PVAc primer layer-mediated coating of silicone implants with a paintable DAC hydrogel. Silicone implants were divided into four zones, visualized by dotted white lines. The images were taken before coating with DAC (A), immediately after coating on zones [i] and [ii] (B), and after the first (C) and the second wash (D) with PBS.

Applying a uniform layer of DAC was challenging, mainly due to the application method and the nature of the pre-formed high-viscosity hydrogel (zone [iii]). However, zones [i] and [ii] can be fully coated *via* painting (Fig. 5B). After the first wash with PBS, DAC coatings on PVAc-primed surfaces remained intact (zone [i]), although some superficial parts were flushed away (Fig. 5C). On the contrary, on the untreated surfaces (zone [ii]), DAC was substantially disengaged from the implant. After the second wash, the remaining DAC hydrogel in zone [ii] was further displaced (Fig. 5D). On the contrary, the hydrogel on the PVAc-primed surface (zone [i]) was still intact. This demonstrated the improved adhesion between the silicone implant surface and the DAC hydrogel provided by the PVAc primer layer, thus demonstrating the stable coating of silicone implants with pre-formed DAC hydrogels. It is noteworthy that DAC residues were still observable on the interface between zones [i] and [ii], which might be stabilized by lateral forces from zone [i] to zone [ii].

The ATR-FTIR difference between zones [iii] and [iv] first confirmed the successful PVAc priming. Secondly, the stable DAC coating was validated by comparing zone [i] to zone [ii]. Same peaks as those from the silicone reference surface (zone [iii]) were observed from zone [ii], indicating an absence of the DAC hydrogel (Fig. 6). On the other hand, on the PVAc-primed surface, the presence of hyaluronic acid (HA) and poly-D,L-lactide (PDLLA) was confirmed (Fig. 6, zone [i]).

More specifically, for HA, broad bands around 3300 cm^{-1} were observed due to the O–H stretching from hydroxyl groups. Additionally, a peak near 1620 cm^{-1} due to the C–O stretching and another around 1400 cm^{-1} corresponding to the carboxylate ion (COO–) asymmetric stretching, as well as additional bands in the range of 1000–1100 cm^{-1} due to the C–O–C stretching vibrations of the sugar backbone, were detected, which is in accordance with the literature studies.[47] For PDLLA, a strong carboxyl stretching mode absorption peak around 1750 cm^{-1} was observed, together with peaks around 1450 cm^{-1} and 1380 cm^{-1} (CH_3

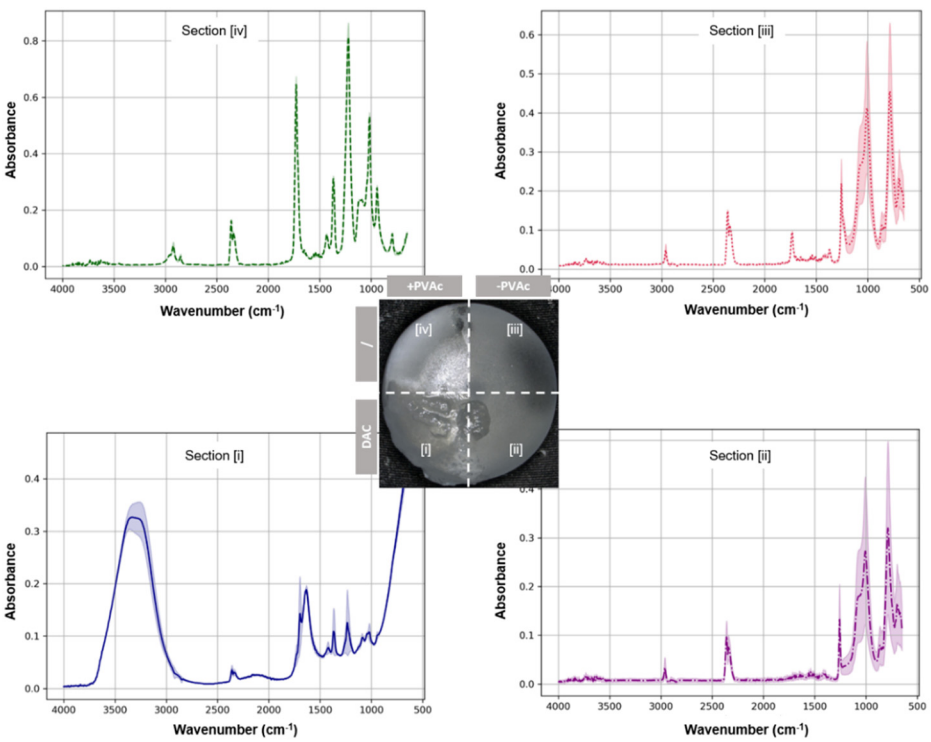

Fig. 6 ATR-FTIR spectra of different implant surface zones after coating zones [i] and [ii] with DAC hydrogels (n = 3).

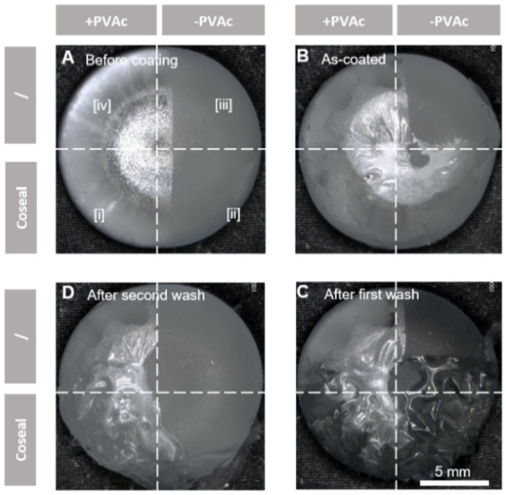

Fig. 7 PVAc primer layer-mediated coating of silicone implants with the sprayable Coseal hydrogel. Silicone implants were divided into four different zones, visualized by dotted white lines. The images were taken before coating with Coseal (A), immediately after coating (B), and after the first (C), and the second wash (D) with PBS.

asymmetric vibration), and a series of bands between 1000 and 1300 cm^{-1} (C–O stretching), in accordance with the literature.[48] Moreover, the absence of PVAc signals from zone [i] suggested no inter-layer mixing of PVAc and DAC, thus confirming a clear demarcation between the hydrogel and the primer layer, and the bridging effect of the PVAc primer layer between the silicone implant surface and a paintable hydrogel.

PVAc-mediated coating of silicone implants with a sprayable hydrogel (Coseal)

In addition to pre-formed hydrogels like DAC, *in situ* formed hydrogels that can be applied to substrate surfaces *via* spraying are also commercially available. Coseal surgical sealant is one of such hydrogels, and its gelation relies on the rapid chemical reactions between 4-arm poly(ethylene glycol) polymers.

After confirming the intact PVAc primer layer on zones [i] and [iv] before hydrogel coating (Fig. 7A), Coseal was sprayed and solidified quickly on the implant surface (~10 seconds), thereby forming a thin coating layer (Fig. 7B). Upon the first washing procedure, it was observed that the Coseal layer remained more stable than DAC, since it was not washed away on both zones [i] and [ii] (Fig. 7C). This indicated the higher structural strength of the Coseal hydrogel due to the covalent nature of crosslinking. Meanwhile, the hydrogel applied directly to the silicone surface (zone [ii]) appeared to swell and detach slightly from the surface. A similar yet less significant phenomenon was visible on the PVAc-primed surface (zone [i]). However, after a second washing process, the Coseal hydrogel layer in zone [ii] completely detached from the surface (Fig. 7D). On the contrary, the hydrogel layer in zone [i] remained on the PVAc-primed surface despite the formation of wrinkles.

The stable coating of the sprayable Coseal hydrogel layer in zone [i] was further confirmed by ATR-FTIR analysis (Fig. 8). Typical PEG characteristics with absorption bands in the 1100 cm^{-1} region (for ether

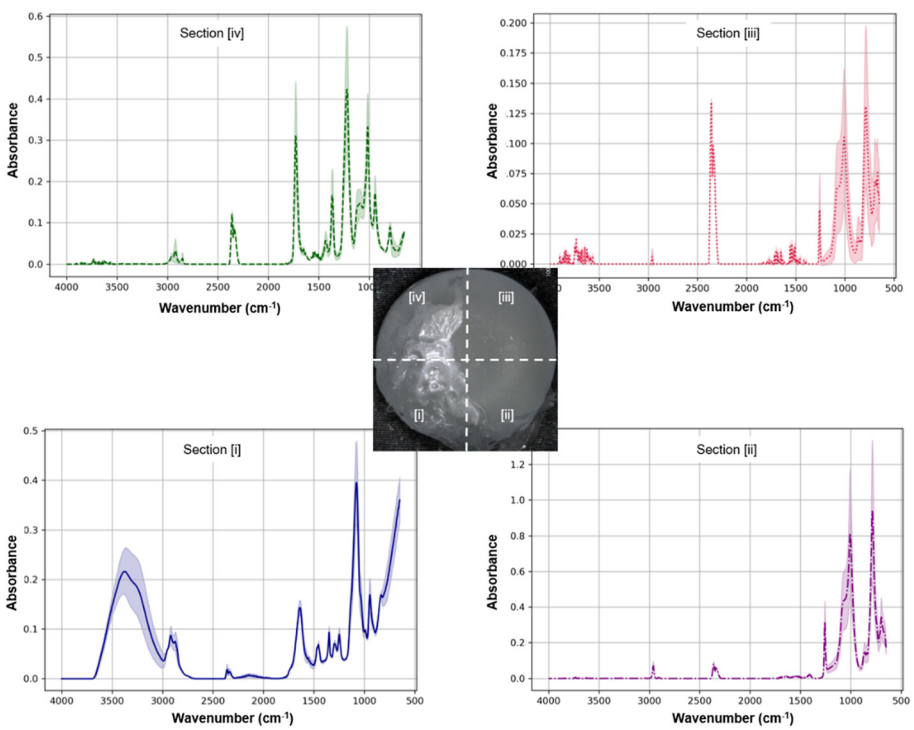

Fig. 8 ATR-FTIR spectra of different implant surface zones taken after coating zones [i] and [ii] with the Coseal hydrogel (n = 3).

linkages C–O–C) was observed, accompanied by the signals around 2850 cm^{-1} (C–H stretching vibrations), and a broad absorption band around 3400 cm^{-1} (O–H stretching vibrations from water absorbed in the hydrogel or hydroxyl groups from PEG).[49] It is noteworthy that the presence of an absorption band at 1730 cm^{-1} (carbonyl groups, C=O) indicated some exposure of PVAc on the coating surface (Fig. 8, zone [i]). This is different from the DAC hydrogel coating (Fig. 6, zone [i]).

Compared to the pre-formed DAC hydrogel, the precursor solution of Coseal was sprayed onto the implant surface. The liquid nature of this formulation prior to *in situ* gelation may facilitate dissolution and diffusion of PVAc polymers, thus resulting in the presence of PVAc in the Coseal layer. Conversely, the non-primed surface (zone [ii]) showed the same peaks as the silicone reference surface (zone [iii]). Changes in signal amplitudes occurred between zones [ii] and [iii], which could be attributed to the residues of the Coseal hydrogel in zone [ii]. Unlike the application of DAC *via* painting, the application of Coseal *via* spraying appeared to be more challenging, with lower spatial accuracy of the target coating. This resulted in coating more than 50% of the implant surface.

Conclusion

Hydrogel coating of implants is an attractive technique to avoid intraoperative contamination during implantation, and thus later development of implant-associated infection. The hydrophobic characteristics of silicone surfaces hinder homogeneous adhesion of hydrogels onto silicone breast implants. To enable stable hydrogel coatings, we established a method to use a stable and cytocompatible PVAc primer layer that straightforwardly improves the wettability of silicone surfaces. This surface priming strategy was proven effective for two commercially available types of hydrogels authorized for internal application, namely, paintable (represented by DAC) and sprayable (represented by Coseal) hydrogels. This method provides opportunities to investigate the hydrogel coating of silicone implants, particularly for preventing infection in breast augmentation and reconstruction with implants. This potential is yet to be confirmed by further *in vivo* experiments. Moreover, in a broader sense, the easy application of hydrogels can render implantable biomaterials with tissue-mimicking interfaces, which could reduce foreign body response.[20]

Data availability

The data supporting this article have been included as part of the ESI.† Data for this paper, including Fig. S1: silicone implants coated directly with the hydrogel; Fig. S2: PVAc primer layer coated on the silicone implant; Fig. S3: FTIR of PVAc primer layer after soaking in PBS (37°) for 7 days; Movie S1_alginate_detachment.avi are available in the ESI.†

Author contributions

Katrin Stanger: conceptualization, funding acquisition, investigation, project administration, resources, and writing – original draft. Dardan Bajrami: conceptualization, data curation, formal analysis, investigation, methodology, project administration, software, validation, visualization, and writing – original draft, review and editing. Fintan Moriarty: writing – review and editing. Peter Wahl: conceptualization, funding acquisition, project administration, supervision, resources, and writing – review and editing. Emanuel Gautier: funding acquisition and writing – review and editing. Alex Dommann: project administration, resources, and writing – review and editing. Kongchang Wei: conceptualization, investigation, methodology, project administration, supervision, visualization, and writing – original draft, review and editing.

Conflicts of interest

The authors declare that there are no conflicts of interest regarding the publication of this paper. All authors have reviewed and approved the manuscript and have agreed to its submission. The authors have no affiliations, financial interests, or personal relationships that could have appeared to influence the work reported in this paper.

Acknowledgements

The Motiva implants for this study were donated by the Establishment Labs Holding Inc. (Alajuela, Costa Rica). The hydrogel DAC for this study was donated by Novagenit, Mezzolombardo, Italy. The hydrogel Coseal was donated by Baxter, Glattpark, Switzerland. The authors thank Mr. Siyuan Tao and Dr. Qun Ren for the helpful discussion.

References

1 J. B. Kim, H. J. Jeon, J. W. Lee, K. Y. Choi, H. Y. Chung, B. C. Cho, S. H. Park, M. H. Park, J. S. Bae and J. D. Yang, *J. Plast. Surg. Hand Surg.*, 2018, **52**, 217–224.
2 T. J. Gampper, H. Khoury, W. Gottlieb and R. F. Morgan, *Ann. Plast. Surg.*, 2007, **59**, 581–590.
3 K. S. Gutowski, E. S. Chwa, J. P. Weissman, S. P. Garg, C. J. Simmons, K. E. Brandt and A. K. Gosain, *Plast. Reconstr. Surg. Glob. Open.*, 2023, **11**, e5486.
4 U. M. Rieger, G. Pierer, N. J. Luscher and A. Trampuz, *Aesthetic Plast. Surg.*, 2009, **33**, 404–408.
5 P. McKinney and G. Tresley, *Plast. Reconstr. Surg.*, 1983, **72**, 27–31.
6 N. Handel, J. A. Jensen, Q. Black, J. R. Waisman and M. J. Silverstein, *Plast. Reconstr. Surg.*, 1995, **96**, 1521–1533.
7 H. Mortada, T. F. AlNojaidi, R. AlRabah, Y. Almohammadi, R. AlKhashan and H. Aljaaly, *Breast J.*, 2022, **2022**, 7857158.
8 H. Panchal and E. Matros, *Plast. Reconstr. Surg.*, 2017, **140**, 7S–13S.

9 G. Giavaresi, E. Meani, M. Sartori, A. Ferrari, D. Bellini, A. C. Sacchetta, J. Meraner, A. Sambri, C. Vocale, V. Sambri, M. Fini and C. L. Romano, *Int. Orthop.*, 2014, **38**, 1505–1512.
10 M. Mozetic, *Materials*, 2019, **12**, 441.
11 E. A. Masters, R. P. Trombetta, K. L. de Mesy Bentley, B. F. Boyce, A. L. Gill, S. R. Gill, K. Nishitani, M. Ishikawa, Y. Morita, H. Ito, S. N. Bello-Irizarry, M. Ninomiya, J. D. Brodell, Jr., C. C. Lee, S. P. Hao, I. Oh, C. Xie, H. A. Awad, J. L. Daiss, J. R. Owen, S. L. Kates, E. M. Schwarz and G. Muthukrishnan, *Bone Res.*, 2019, **7**, 20.
12 M. Gimeno, P. Pinczowski, M. Perez, A. Giorello, M. A. Martinez, J. Santamaria, M. Arruebo and L. Lujan, *Eur. J. Pharm. Biopharm.*, 2015, **96**, 264–271.
13 L. Tang, P. Thevenot and W. Hu, *Curr. Top. Med. Chem.*, 2008, **8**, 270–280.
14 M. Lam, V. Migonney and C. Falentin-Daudre, *Acta Biomater.*, 2021, **121**, 68–88.
15 B. H. Shin, B. H. Kim, S. Kim, K. Lee, Y. B. Choy and C. Y. Heo, *Biomater. Res.*, 2018, **22**, 37.
16 J. E. Baker, A. P. Seitz, R. M. Boudreau, M. J. Skinner, A. Beydoun, N. Kaval, C. C. Caldwell, E. Gulbins, M. J. Edwards and R. M. Gobble, *Plast. Reconstr. Surg.*, 2020, **146**, 1029–1041.
17 J. van Heerden, M. Turner, D. Hoffmann and J. Moolman, *J. Plast. Reconstr. Aesthet. Surg.*, 2009, **62**, 610–617.
18 A. Mendonça Munhoz, F. Santanelli di Pompeo and R. De Mezerville, *Case Reports in Plastic Surgery & Hand Surgery*, 2017, **4**, 99–113.
19 J. C. Doloff, O. Veiseh, R. de Mezerville, M. Sforza, T. A. Perry, J. Haupt, M. Jamiel, C. Chambers, A. Nash, S. Aghlara-Fotovat, J. L. Stelzel, S. J. Bauer, S. Y. Neshat, J. Hancock, N. A. Romero, Y. E. Hidalgo, I. M. Leiva, A. M. Munhoz, A. Bayat, B. M. Kinney, H. C. Hodges, R. N. Miranda, M. W. Clemens and R. Langer, *Nat. Biomed. Eng.*, 2021, **5**, 1115–1130.
20 J. Wu, J. Deng, G. Theocharidis, T. L. Sarrafian, L. G. Griffiths, R. T. Bronson, A. Veves, J. Chen, H. Yuk and X. Zhao, *Nature*, 2024, **630**, 360–367.
21 Y. Barnea, D. C. Hammond, Y. Geffen, S. Navon-Venezia and K. Goldberg, *Aesthetic Surg. J.*, 2018, **38**, 1188–1196.
22 S. H. Kang, C. Sutthiwanjampa, H. S. Kim, C. Y. Heo, M. K. Kim, H. K. Kim, T. H. Bae, S. H. Chang, W. S. Kim and H. Park, *J. Ind. Eng. Chem.*, 2021, **97**, 226–238.
23 S. Finnegan and S. L. Percival, *Adv. Wound Care*, 2015, **4**, 398–406.
24 C. Weller and G. Sussman, *J. Pharm. Pract. Res.*, 2006, **36**, 318–324.
25 P. M. Vogt, K. Reimer, J. Hauser, O. Rossbach, H. U. Steinau, B. Bosse, S. Muller, T. Schmidt and W. Fleischer, *Burns*, 2006, **32**, 698–705.
26 Z. Cao, Y. Luo, Z. Li, L. Tan, X. Liu, C. Li, Y. Zheng, Z. Cui, K. W. K. Yeung, Y. Liang, S. Zhu and S. Wu, *Macromol. Biosci.*, 2021, **21**, e2000252.
27 W. Xu, S. Dong, Y. Han, S. Li and Y. Liu, *Curr. Pharm. Des.*, 2018, **24**, 843–854.
28 K. Yang, Q. Han, B. Chen, Y. Zheng, K. Zhang, Q. Li and J. Wang, *Int. J. Nanomed.*, 2018, **13**, 2217–2263.
29 L. Drago, W. Boot, K. Dimas, K. Malizos, G. M. Hänsch, J. Stuyck, D. Gawlitta and C. L. Romanò, *Clin. Orthop. Relat. Res.*, 2014, **472**, 3311–3323.
30 K. Tsikopoulos, A. Bidossi, L. Drago, D. R. Petrenyov, P. Givissis, D. Mavridis and P. Papaioannidou, *Clin. Orthop. Relat. Res.*, 2019, **477**, 1736–1746.
31 A. G. Gristina, *Science*, 1987, **237**, 1588–1595.
32 D. B. McConda, J. M. Karnes, T. Hamza and B. A. Lindsey, *Biofouling*, 2016, **32**, 627–634.
33 G. Subbiahdoss, R. Kuijer, D. W. Grijpma, H. C. van der Mei and H. J. Busscher, *Acta Biomater.*, 2009, **5**, 1399–1404.
34 G. Subbiahdoss, I. C. Fernández, J. F. Domingues, R. Kuijer, H. C. van der Mei and H. J. Busscher, *PLoS One*, 2011, **6**, e24827.
35 G. Giammona, P. Giovanna, S. Palumbo Fabio, S. Maraldi, S. Scarponi and L. Romanò Carlo, in *Hydrogels*, ed. H. Sajjad and H. Adnan, IntechOpen, Rijeka, 2018, ch. 9, DOI: **10.5772/intechopen.73203**.
36 K. Malizos, M. Blauth, A. Danita, N. Capuano, R. Mezzoprete, N. Logoluso, L. Drago and C. L. Romano, *J. Orthop. Trauma*, 2017, **18**, 159–169.
37 C. L. Romanò, E. De Vecchi, M. Bortolin, I. Morelli and L. Drago, *J. Bone Jt. Infect.*, 2017, **2**, 63–72.
38 M. J. Owen, *Macromol. Rapid Commun.*, 2021, **42**, e2000360.
39 M. Lam, V. Migonney and C. Falentin-Daudre, *Acta Biomater.*, 2021, **121**, 68–88.
40 L. Cheng, C. Liu, J. Wang, Y. Wang, W. Zha and X. Li, *ACS Appl. Polym. Mater.*, 2022, **4**, 3462–3472.
41 M. Jannesari, J. Varshosaz, M. Morshed and M. Zamani, *Int. J. Nanomed.*, 2011, **6**, 993–1003.
42 G. A. Gonzalez Novoa, J. Heinamaki, S. Mirza, O. Antikainen, A. I. Colarte, A. S. Paz and J. Yliruusi, *Eur. J. Pharm. Biopharm.*, 2005, **59**, 343–350.
43 H. G. Jeong, Y. E. Kim and Y. J. Kim, *Macromol. Res.*, 2013, **21**, 1233–1240.
44 K. Y. Lee and D. J. Mooney, *Prog. Polym. Sci.*, 2012, **37**, 106–126.
45 Q. Xiao, X. Gu and S. Tan, *Food Chem.*, 2014, **164**, 179–184.
46 M. Franceschini, N. A. Sandiford, V. Cerbone, L. C. T. Araujo and D. Kendoff, *HIP Int.*, 2020, **30**, 7–11.
47 M. Al-Sibani, A. Al-Harrasi and R. H. H. Neubert, *Pharmazie*, 2017, **72**, 81–86.
48 R. D. Pereira, G. V. Salmoria, M. O. C. de Moura, A. Aragones and M. C. Fredel, *Mater. Res.*, 2014, **17**, 33–38.
49 H. Shinzawa, T. Uchimaru, J. Mizukado and S. G. Kazarian, *Vib. Spectrosc.*, 2017, **88**, 49–55.